ELSEVIER

www.elsevier.nl/locate/carres

Carbohydrate Research 317 (1999) 145–154

CARBOHYDRATE RESEARCH

FTIR spectroscopy as a tool for the analysis of olive pulp cell-wall polysaccharide extracts

Manuel A. Coimbra [a,*], António Barros [b], Douglas N. Rutledge [b], Ivonne Delgadillo [a]

[a] *Department of Chemistry, University of Aveiro, P-3810 Aveiro, Portugal*
[b] *Institut National Agronomique Paris-Grignon, Laboratoire de Chimie Analytique, 16 rue Claude Bernard, F-75005 Paris, France*

Received 9 December 1998; accepted 15 March 1999

Abstract

The sequential extraction of olive pulp cell-wall material (CWM) and its subsequent fractionation by ethanol precipitation and anion-exchange chromatography gave a wide range of cell-wall polysaccharide fractions, characterised by sugar analysis. Several multivariate procedures, such as principal component analysis (PCA), trimmed object projections (TOP), canonical correlation analysis (CCA), and partial least squares regression (PLS), were applied to their FTIR spectra, in the region between 1200 and 850 cm^{-1}. The combination of these chemometric techniques along with the chemical information allowed the type of polymers present to be distinguished: pectic polysaccharides rich in uronic acid, pectic polysaccharides rich in arabinose, arabinose-rich glycoproteins, xyloglucans, and glucuronoxylans. It was also possible to highlight the most important and characteristic wavenumbers for each type of polymer present. A calibration model for the quantification of xylose residues of the hemicellulosic polysaccharides was proposed. The high diversity of samples used and their characteristic features allowed models to be obtained, using a very expeditious methodology, that represent a realistic description of the olive pulp cell-wall polymers.

Keywords: Olive pulp; Cell walls; FTIR spectroscopy; PCA; Pectic polysaccharides; Hemicelluloses; Glucuronoxylans; Xylose

1. Introduction

IR spectroscopy has been proposed for monitoring cell-wall extraction [1], as well as cell-wall changes during processing and quality control of vegetable processing [2]. In combination with multivariate analysis, on the basis of the characteristic spectra, FTIR spectroscopy has been used for the distinction of apple from other fruits and vegetable cell walls [3,4], and screening for *Arabidopsis* cell-wall mutants [5]. The application of FTIR spectroscopy to the study of cell-wall polysaccharides has proved to be a very valuable technique for the study of cell-wall monosaccharide composition. Recently, uronic acid and neutral sugars of pectic origin from olive and orange cell walls were quantified using the spectral region between 1200 and 850 cm^{-1} [6].

Plant cell-wall neutral sugars such as Ara, Xyl, Glc or Man, the main constituents of pectic and hemicellulosic polysaccharides, are usually quantified after acid hydrolysis and derivatisation to alditol acetates by gas chromatography [7,8]. Uronic acids are usually quantified, after the polymer hydrolysis, by colorimetric methods that involve the reaction with m-hydroxydiphenyl in concentrated sulfuric acid media [9,10] or by HPLC [11–13].

* Corresponding author. Fax: +351-34-370084.
E-mail address: mac@dq.ua.pt (M.A. Coimbra)

0008-6215/99/$ - see front matter
PII: S0008-6215(99)00071-3

These analyses, involving hydrolysis, are time consuming and expensive. The possibility of using FTIR spectroscopy for monitoring the cell-wall monosaccharide composition and, as a consequence, the type of polysaccharides present in the different fractions obtained during the study of the cell-wall material (CWM), represent an important improvement in comparison with the traditional chemical/instrumental methods. The acquisition of the FTIR spectra and the application of the appropriate statistical model is rapid and is, by far, less expensive and more environmentally friendly than the chemical methods. On the other hand, FTIR spectroscopy allows analysis of the samples without needing to perform sugar hydrolysis, which usually leads to difficulties in obtaining quantitative results [7,12,14].

The sequential extraction of olive pulp CWM and its subsequent fractionation by ethanol precipitation and anion-exchange chromatography gave a wide range of fractions rich in cell-wall polysaccharides [8,15]. Following the work carried out on the identification and quantification of uronic acid and neutral sugars of pectic origin from olive and orange cell walls in the spectral region between 1200 and 850 cm^{-1} [6], this paper shows the potential of FTIR spectroscopy associated with the appropriate chemometric methods to discriminate olive pulp cell-wall polysaccharides and allow the quantification of Xyl in hemicellulosic samples. The final intention of these studies is: (a) to be able to predict the type of polysaccharides according to their spectra; (b) to quantify the main type of constituent monosaccharide residues present in the samples; and (c) to study the possibility of extrapolating the results to more complex systems such as the whole CWM and the intact vegetal tissue. This information will allow an expeditious assessment and the monitoring of the polysaccharide modifications that occur during olive ripening and/or processing for table olives and olive oil extraction purposes.

2. Experimental

Sample origin.—CWM was prepared from olive pulp and sequentially extracted with aqueous solutions following the methods described by Coimbra et al. [8,16]. The CWM (1 g) was sequentially extracted with (i) 50 mM *trans*-1,2-cyclohexane-diamine-*N*,*N*,*N*′,*N*′-tetraacetate, Na salt (CDTA), 100 mL, pH 6.5 at 20 °C for 6 h (CDTA-1); (ii) 50 mM CDTA (100 mL), pH 6.5 at 20 °C for 2 h (CDTA-2); (iii) 50 mM Na_2CO_3 + 20 mM $NaBH_4$ (100 mL) at 1 °C for 16 h (Na_2CO_3-1); (iv) 50 mM Na_2CO_3 + 20 mM $NaBH_4$ (100 mL) at 20 °C for 3 h (Na_2CO_3-2); (v) 1 M KOH + 20 mM $NaBH_4$ (75 mL) at 1 °C for 2 h (KOH-1); (vi) 1 M KOH + 20 mM $NaBH_4$ (75 mL) at 20 °C for 2 h (KOH-2); (vii) 4 M KOH + 20 mM $NaBH_4$ (75 mL) at 20 °C for 2 h (KOH-3); and (viii) 4 M KOH + 3.5% H_3BO_3 + 20 mM $NaBH_4$ (75 mL) at 20 °C for 2 h (KOH-4). The alkali extractions were carried out with O_2-free solutions under argon. After each extraction, solubilised polymers were separated from the insoluble residue by centrifugation (CDTA and Na_2CO_3 extracts) or by filtration through G1 glass sinter (KOH extracts). All extracts were filtered through GF/C and dialysed exhaustively; Na_2CO_3 and KOH extracts were acidified to pH 5 with acetic acid prior to dialysis. Precipitates formed during dialysis of alkali extracts were collected separately. The cellulose-rich residues (CR) remaining after the final alkali extraction (4 M KOH + borate) were suspended in water (25 mL) and the solutions were acidified to pH 5 and dialysed. The supernatants of the CR dialysis were collected separately by centrifugation from the CR1 residue. All extracts collected after dialysis were concentrated and freeze-dried. In order to have a wide range of separated polymers, several selected fractions were submitted to graded precipitation with ethanol. The polymers were dissolved in water and precipitated by the addition of ethanol, as described by Coimbra et al. [16]. Some fractions were submitted to anion-exchange chromatography, DEAE-trisacryl M columns, as described by Redgwell and Selvendran [17].

Carbohydrate analysis.—Neutral sugars were released by Saeman hydrolysis [18] and analysed as their alditol acetates by GLC [19,20] using a Hewlett–Packard 5890 with a

split injector (split ratio 1:60) and an FID detector. A 25 m CP-Sil-43 CB column, with I.D. 0.15 and 0.20 μm film thicknesses was used. With the injector and detector operating at 220 °C, the following temperature program was used: 180 °C for 5 min and 200 °C for 20 min, with a rate of 0.5 °C/min. Linear velocity of the carrier gas (H_2) was set at 50 cm/s at 200 °C. Uronic acids were determined colorimetrically by a modification [8] of the Blumenkrantz and Asboe-Hansen [9] method.

FTIR spectra.—FTIR spectra of the pectic materials were obtained at a resolution of 8 cm^{-1}. The samples, in triplicate, were incorporated into KBr (spectroscopic grade) and pressed into a 1 mm pellet. Spectra were recorded in the absorbance mode from 4000 to 400 cm^{-1} using a Nicolet Magna-IR 550.

Data pre-treatment.—Each spectrum was baseline corrected and the absorbance was normalised between 0 and 1. The spectra were transferred via a JCAMP.DX format [21] into the data analysis software package developed in our laboratories.

Principal component analysis.—Principal component analysis (PCA) is one of the most often used chemometric methods for data reduction and exploratory analysis on high-dimensional data sets. The main goal of PCA is to obtain a small set of principal components (latent variables) that contain most of the variability on these data sets. The new sub-space defined by these principal components leads to a model that is easier to interpret than the original data set. From these results, it should be possible to highlight several characteristics and correlate them to the physico-chemical proprieties of samples [22].

Canonical correlation analysis.—Canonical correlation analysis (CCA) is a method that makes it possible to study simultaneously two different sets of variables measured on the same samples. It considers the correlation between the two sets and highlights the most correlated ones. It helps to establish a relationship between the two groups, thus allowing the detection of those variables that change in the same way. This method is useful to analyse and characterise one group of variables about which there is little or no information, by relating it to another group of well-understood and well-characterised variables [23].

Trimmed object projection.—Trimmed object projection (TOP) is a non-parametric latent structure decomposition method based on object projections. The main goal of this procedure is to find directions in the multivariate space that represent the major body of the data set without the constraints of the classic PCA that maximise the variance of the data set and, hence, is very sensible to the presence of atypical samples (outliers). This technique is generally based on the concept of trimmed principal objects that represent the major part of the objects and, at the same time, are unaffected by outliers. The contribution of each object is weighted according to a threshold that is based on the distance of each object to a median centre point. This procedure provides robust principal components which are, therefore, resistant to the presence of outliers in data sets [24].

Partial least squares regression.—Partial least squares regression (PLS) is a procedure used to model the relationship between a set of predictor variables X (N objects $\times$ K variables) and a set of response variables Y (N objects $\times$ M responses). In this study there is only one response in Y (concentration), thus Y has N (objects) $\times$ 1 (response) dimensions [25]. This procedure was applied to construct calibration models for quantification of xylose residues in olive pulp hemicelluloses using FTIR spectroscopy. Usually, the IR spectra obtained in many studies involve the use of many wavelengths (or wavenumbers) as opposed to the number of observations. The PLS regression procedure has the advantage of accepting more variables than objects in the data and of avoiding the problem of collinearity among variables. The presence of non-linearities, and the fact that normally the spectra obtained have more than one component involved in the analysis, leads to the need for regression procedures such as PLS. However, it is desirable to find a method that can highlight those wavelengths that are highly selective for the component to be characterised.

Cross validation–leave-one-out.—In this study, the determination of the number of factors for the application of PLS1 regression was based on the leave-one-out cross validation procedure. Since for almost all the samples there are three spectra replicates, the leave-one-out procedure removes each time all the replicates of each sample.

3. Results and discussion

Selection of samples.—Table 1 shows the origin and sugars composition of 63 cell-wall fractions. These samples had been chemically characterised previously by Coimbra et al. [8,15]. Three data sets were used for the multivariate analysis (Table 1, column 2). Data set 1 used a small amount of selected pectic and hemicellulosic fractions, 14 samples, 42 spectra of pectic polysaccharides and 9 samples, 26 spectra of hemicellulosic polysaccharides, for a total of 68 spectra from 23 samples (all samples, except one, were analysed in triplicate). Data set 2 used all cell-wall samples, 188 spectra from 63 fractions. Data set 3 used only the hemicellulosic and cellulosic samples, that is the fractions obtained with KOH solutions or after chlorite treatment plus the cellulosic and final residues, for a total of 122 spectra from 41 samples.

Olive pulp pectic polysaccharides are characterised by the presence of residues of hexuronic acid (HexA), Ara, Gal and Rha. In the samples used, HexA and Ara vary considerably. Olive pulp hemicellulosic polysaccharides are characterised by the presence of Xyl, Glc, HexA, and also Gal. Xyl and HexA are characteristic of glucuronoxylans, and Glc, Xyl and Gal are characteristic of xyloglucans [15]. The hemicellulosic samples used for selection in data set 1 were composed of pure glucuronoxylans, or of mixtures of glucuronoxylans and xyloglucans; some fractions contain also small amounts of pectic polysaccharides rich in Ara.

FTIR spectra.—Fig. 1 shows two FTIR spectra: Fig. 1(a) represents a spectrum of a pectic polysaccharide sample rich in UA and Fig. 1(b) a hemicellulosic sample rich in glucuronoxylans. The spectra show high absorbance at wavenumbers characteristic of cell-wall polysaccharides [1]: 3440 cm^{-1} OH, 1750 cm^{-1} ester, 1630 cm^{-1} carboxylate and 1200–850 cm^{-1} carbohydrate. Major differences in both spectra are due to the ester band, that is absent in hemicellulosic polymers, as they were extracted with alkali solutions, and to the carbohydrate bands. A closer look at the 1200–850 cm^{-1} region (Fig. 2) of a large number of pectic (Fig. 2(a)) and hemicellulosic (Fig. 2(b)) polysaccharide fractions shows that the two types of samples have different spectral patterns. In order to verify, in the internal data structure, if this region is useful for the distinction of these cell-wall polymers, the spectra were analysed by different multivariate analysis procedures.

Distinction between pectic and hemicellulosic polysaccharides. (a) PCA.—The scores plot of the PCA performed to the data set 1 is shown in Fig. 3(a). PC1, which contains 51% of the data-set variability, allows the two types of

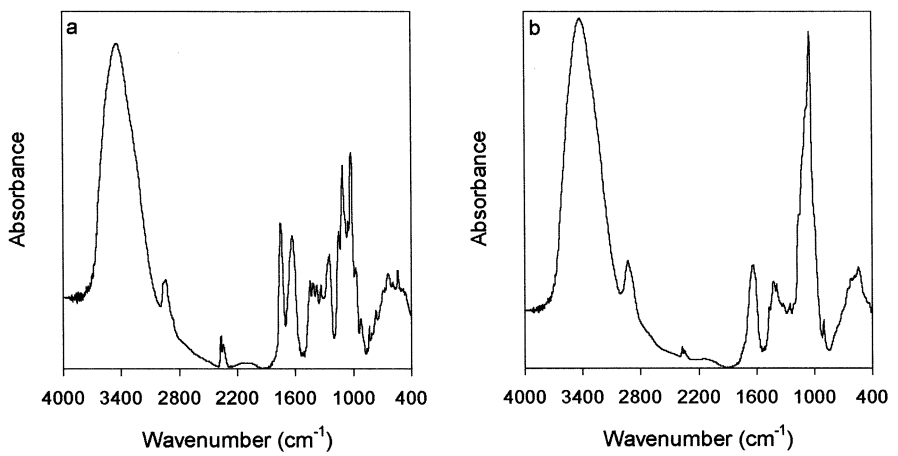

Fig. 1. FTIR spectra in the 4000–400 cm^{-1} region of (a) pectic polysaccharides; and (b) hemicellulosic polysaccharides.

Table 1
Origin and sugars composition of olive pulp cell-wall fractions

Origin	Data Set	mol%								Total sugar (mg/g)
		Rha	Fuc	Ara	Xyl	Man	Gal	Glc	HexA	
Cell Wall Material	2	1	0	27	12	2	3	29	26	619
CDTA-1	2	1	0	11	0	0	1	1	86	753
CDTA-1 A	1 2	1	0	18	0	1	1	1	78	750
CDTA-1 B	1 2	1	0	19	0	0	1	1	78	634
CDTA-1 C	1 2	1	0	9	0	0	1	1	88	668
CDTA-1 A1	2	2	0	20	1	1	1	5	70	824
CDTA-1 Et60	1 2	2	0	29	0	0	1	1	67	472
CDTA-1 Et75	1 2	3	0	25	0	0	2	1	69	615
CDTA-1 Et85	1 2	2	0	29	1	0	1	2	65	586
CDTA-2 ppt	2	3	0	45	1	0	2	1	48	523
Na_2CO_3-1	1 2	2	0	40	1	0	3	1	53	767
Na_2CO_3-1 ppt	1 2	2	0	41	1	0	3	3	50	495
Na_2CO_3-1 Et70	1 2	1	2	36	0	0	2	1	59	914
Na_2CO_3-1 B	2	3	0	71	1	0	4	2	19	581
Na_2CO_3-1 C1	2	3	0	68	0	0	3	1	25	804
Na_2CO_3-1 C2	2	2	0	12	1	1	2	1	81	590
Na_2CO_3-1 D	2	1	0	17	1	1	2	2	76	695
Na_2CO_3-2	1 2	1	0	52	1	0	2	1	44	882
KOH-1 sn	2 3	1	0	27	31	1	5	13	22	789
KOH-1 ppt	2 3	1	0	8	67	2	2	7	13	547
KOH-2 sn	2 3	1	0	48	8	9	7	13	14	471
KOH-2 ppt	2 3	1	0	10	53	2	2	14	18	368
KOH-1 sn Et50	1 2 3	1	1	15	32	1	9	34	7	904
KOH-1 sn Et75	1 2 3	1	0	13	50	2	4	13	17	929
KOH-1 sn Et75 A	1 2 3	1	0	9	62	2	4	13	9	835
KOH-1 sn Et75 B-D	1 2 3	1	0	16	52	2	4	13	12	780
KOH-1 sn 1M Et30	1 2 3	1	0	16	56	1	4	15	7	907
KOH-1 sn 1M Et50	1 2 3	1	0	17	36	9	9	24	4	913
KOH-1 sn RI	2 3	3	0	69	2	0	5	3	18	849
KOH-1 sn 2M Et50	2 3	2	0	42	29	1	5	11	10	852
KOH-1 sn 1M Et30 ppt	2 3	1	1	4	75	0	1	3	15	858
KOH-1 sn 1M Et30 B	2 3	2	1	48	26	0	4	4	15	549
KOH-1 sn 1M Et30 C	2 3	3	1	60	11	1	5	5	14	593
KOH-1 sn 1M Et30 A ppt	2 3	2	1	21	49	0	3	10	14	752
KOH-1 sn 1M Et30 A1	2 3	1	1	24	55	0	3	2	14	687
KOH-1 sn 1M Et30 A2	2 3	1	1	8	51	1	6	26	6	858
KOH-1 sn 1M Et30 A3	2 3	1	0	6	54	8	5	19	7	553
KOH-1 sn 1M Et30 A4	2 3	2	0	6	63	2	4	10	13	436
KOH-1 sn 1M Et30 A5	2 3	3	0	32	45	0	2	3	15	719
KOH-1 ppt A	1 2 3	1	0	1	91	0	0	1	6	923
KOH-1 ppt A K10	1 2 3	1	0	1	87	0	0	2	9	869
KOH-1 ppt A K6	1 2 3	2	0	3	78	1	1	4	11	821
KOH-3 sn	2 3	0	1	15	25	11	10	30	8	936
KOH-4 sn	2 3	1	0	64	5	5	5	8	13	588
KOH-3 sn RI	2 3	1	0	32	21	9	6	20	11	590
KOH-3 sn A	2 3	1	1	41	5	18	9	21	4	509
KOH-4 sn A	2 3	1	0	66	3	10	6	10	4	679
KOH-4 sn B	2 3	2	0	76	2	1	3	4	12	635
KOH-4 sn C	2 3	3	0	62	2	0	4	5	24	561
sn-CR	1 2	2	0	53	1	0	3	1	40	936
sn-CR ppt	1 2	2	0	73	0	0	3	0	22	803
sn-CR Et60	1 2	2	0	73	1	0	3	0	21	1028
sn-CR Et85	1 2	2	0	78	0	0	2	0	18	863
Cellulosic Residue	2 3	1	0	18	8	1	2	56	14	722
Chlorite	2 3	3	0	56	1	0	4	1	35	732
Chlorite ppt	2 3	2	0	71	1	0	4	3	19	712
Chlorite A	2 3	1	0	80	2	0	3	2	12	858
Chlorite B	2 3	2	0	72	1	0	5	2	18	861
Chlorite C	2 3	2	0	74	1	0	3	0	20	838
Chlorite KOH	2 3	2	0	48	16	2	5	9	18	505
Chlorite KOH A	2 3	0	0	19	14	21	12	29	5	630
Chlorite KOH B	2 3	2	0	62	5	1	5	8	17	618
Final Residue	2 3	1	0	6	7	2	1	78	5	725

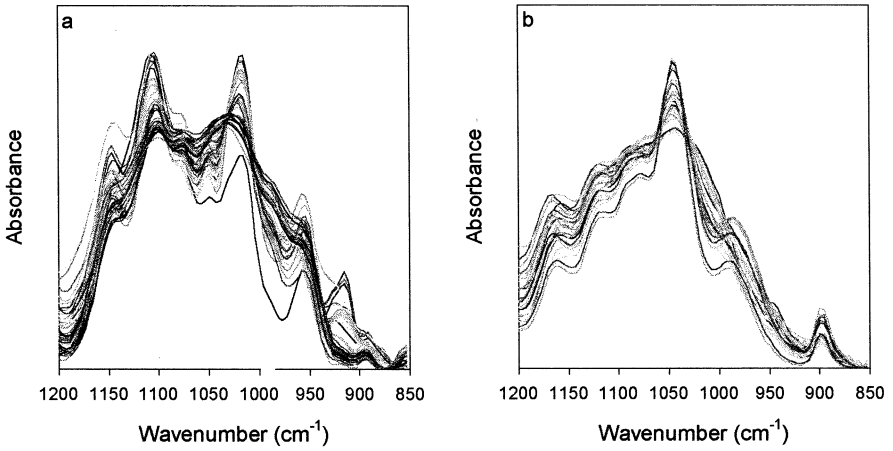

Fig. 2. FTIR spectra in the 1200–850 cm^{-1} region of all (a) pectic polysaccharides; and (b) hemicellulosic polysaccharides.

polysaccharide to be distinguished. The data also show that PC2 (27%), for the hemicellulosic samples, is associated with Xyl content; for the pectic samples, it is associated with Ara content. Fig. 4(a) shows the loading plots of PC1 and PC2. The loadings shows which are the most important wavenumbers that explain the distinction. PC1 loadings show that the hemicellulosic samples (negative values) are characterised mainly by the 1173 and 1041 cm^{-1} wavenumbers. Pectic samples (positive values) are characterised mainly by the wavenumbers 1145, 1104, 1014 and 952 cm^{-1}. Those wavenumbers were recently identified as regions of high absorbance for exA of pectic origin [6].

Distinction between pectic and hemicellulosic polysaccharides. (b) TOP.—The application of TOP to data set 1 allowed a distinction in PC1 between pectic and hemicellulosic samples, as occurred with PCA analysis (Fig. 3(b)). Also, as for the PCA, for pectic polysaccharides, PC2 allows the distinction of the fractions according to their content in Ara, and, for hemicellulosic polysaccharides, according to their content in Xyl. Moreover, the scores scatter plot was more informative and allowed five groups to be obtained, corresponding to the different olive pulp cell-wall polymers in extracts: CDTA, Na_2CO_3-1, Na_2CO_3-2 + sn-CR, KOH-1 sn, and KOH-1 ppt. As shown in Table 1, CDTA-1 samples are the UA-richest pectic fractions; the fractions with the lowest content in HexA are the Na_2CO_3-2 + sn-CR. Na_2CO_3-1 extracts showed intermediate pectic polysaccharide composition. KOH-1 ppt fractions are composed mainly of Xyl and also contain HexA, and KOH-1 sn fractions have lower amounts of Xyl, and also contain Glc, Ara, Gal, and minor amounts of other sugar residues. PC1 loadings (Fig. 4(b)) indicate that pectic polysaccharides are characterised mainly by the wavenumbers 1104, 1014, 984 and 952 cm^{-1}; the hemicellulosic polysaccharides are characterised mainly by the wavenumbers 1173, 1126, 1061–1041 and 902 cm^{-1}. PC2 loadings indicate that pectic polysaccharides extracted with CDTA are characterised mainly by the wavenumbers 1145, 1104 and 1014 cm^{-1}; the hemicellulosic polysaccharides obtained in the extract KOH-1 ppt are characterised mainly by the wavenumbers 1041, 984 and 945 cm^{-1}. PC2 confirms the importance of the 1104 and 1014 cm^{-1} as diagnostic wavenumbers for the characterisation of pectic polysaccharides rich in UA and the wavenumber 1041 cm^{-1} for the characterisation of the glucuronoxylans present in KOH-1 ppt extract.

Application of TOP for distinction of olive pulp cell-wall polysaccharides.—In order to evaluate the potential of both TOP and the wavenumber region 1200–850 cm^{-1} in the distinction of the type of olive pulp cell-wall polymers, a large number of samples (data set 2) were analysed. Fig. 3(c) shows the scores scatter plot of PC1 × PC3 (no identifiable structure was obtained in PC2). A close look at the distribution of the samples in the plot allowed the identification of five distinct

groups, according to the major type of polymers present. PC1 is related to the differences between pectic polysaccharides (PPS rich in Ara and PPS rich in HexA) and glucuronoxylans. PC3 is related to the differences between pectic polysaccharides rich in HexA and all other polymers. PC1 and PC3 loadings (Fig. 4(c)) confirm the wavenumbers characteristic of pectic and hemicellulosic polysaccharides. This large data set allows the inference that the major distinction obtained by FTIR spectroscopy in the 1200–850 cm^{-1} region occurs between the pectic polysaccharides rich in exA and glucuronoxylans. The amount of Ara present in pectic samples is also able to contribute to the distinction between the polymers. Although PC1 is not able to make that distinction, it is possible in PC3. PC1 also allows the distinction of samples containing pectic polysaccharides rich in Ara from those that contain Ara arising from glycoproteins. This type of glycoprotein is rich in hydroxyproline and is usually present in 4 M KOH cell-wall extracts [15]. These polymers can also be discriminated by PC1 from the mixtures of water-soluble xylans and xyloglucans, and from the glucuronoxylans.

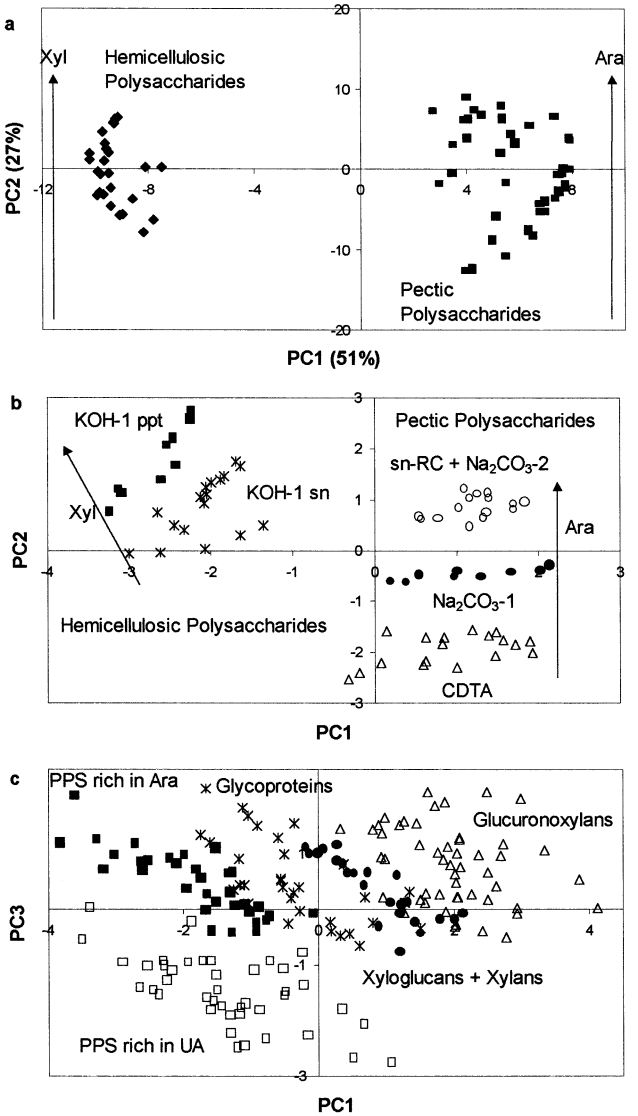

Fig. 3. Scores scatter plots: (a) PCA data set 1; (b) TOP data set 1; and (c) TOP data set 2.

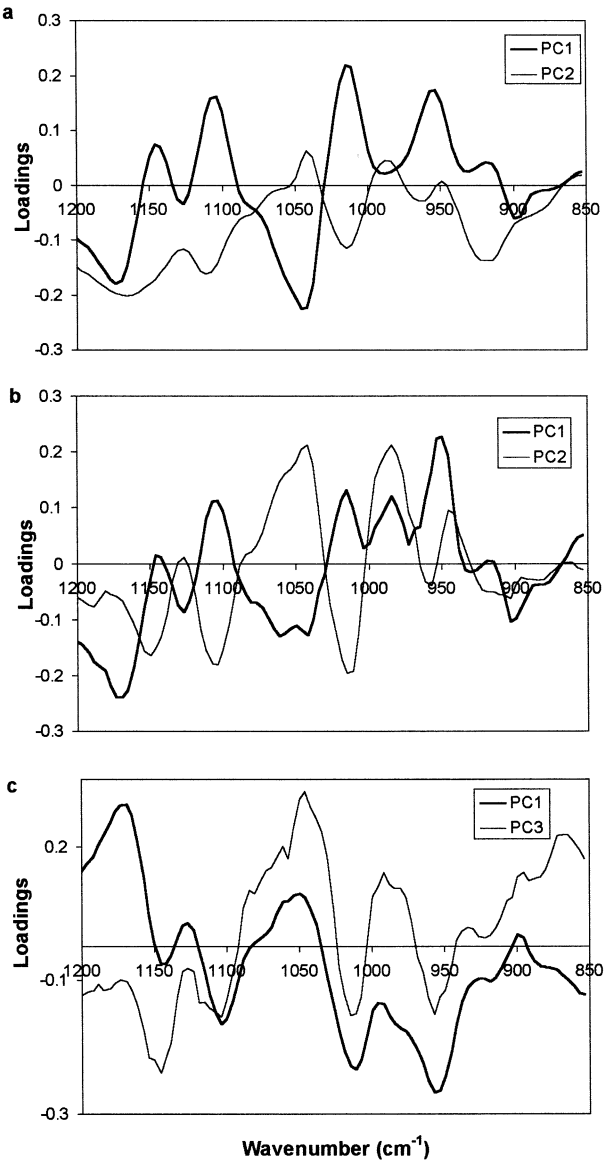

Fig. 4. Loadings plots: (a) PC1 and PC2 from PCA data set 1; (b) PC1 and PC2 from TOP data set 1; and (c) PC1 and PC3 from TOP data set 2.

Canonical correlation analysis for distinction of olive pulp cell-wall polysaccharides.—Fig. 5(a) shows the CCA similarity map of the

spectra in the region 1200–850 cm^{-1} and samples sugars composition from data set 2. It is possible to observe three clusters containing: pectic polysaccharides rich in exA; polymers rich in Ara (pectic polysaccharides and glycoproteins); and hemicellulosic polysaccharides (glucuronoxylans, xyloglucans, and also the CWM and the cellulosic residues). Fig. 5(b) shows the CCA loadings of the sugars composition data matrix. CV1 is correlated positively with HexA and negatively with Xyl. Comparing Fig. 5(a) and (b), it can be seen

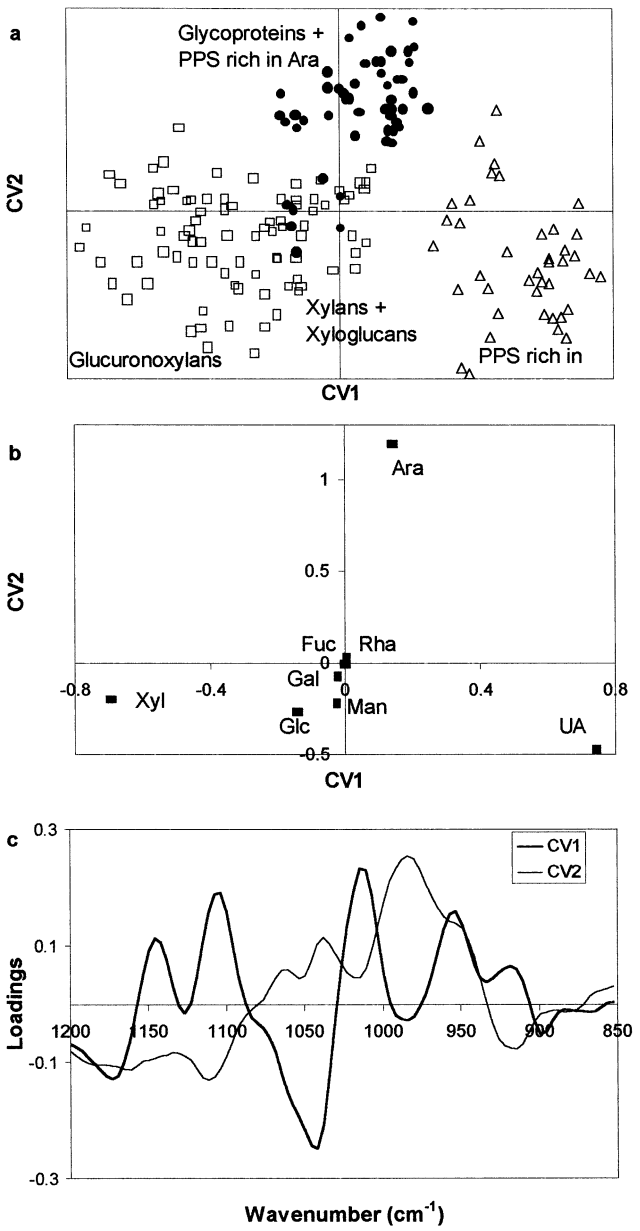

Fig. 5. CCA of data set 2: (a) scores of the spectral data matrix; (b) loadings of the sugars composition data matrix; and (c) loadings of the spectral data mix.

that the HexA of pectic origin (galacturonic acid) and the Xyl of glucuronoxylans are responsible for the distinction of the FTIR spectra of these cell-wall polymers; the CV1 correlation between the two domains is 0.96. CV2 is correlated with Ara and is not significantly related with any other sugars. In fact, the CV2 correlation between the two domains is weak (0.74). Fig. 5(c) shows the CCA loadings of the FTIR spectra data matrix. It can be seen that the wavenumbers characteristic for the distinction of galacturonic acid are 1145, 1104, 1014 and 952 cm^{-1}; the wavenumbers characteristic for the distinction of Xyl are 1173 and 1041 cm^{-1}; and the wavenumbers characteristic for the distinction of Ara are 1065, 1038, 984 and 952 cm^{-1}. These results are in accordance with those previously reported by Coimbra et al. [6] for galacturonic acid and Ara of pectic origin.

CCA for distinction of olive pulp hemicellulosic polysaccharides.—In order to try to identify more precisely the absorbance of the hemicellulosic polysaccharides in the 1200–850 cm^{-1} region of the FTIR spectra, a CCA was applied to the hemicelluloses set (data set 3). Fig. 6(a) shows the CCA similarity map of the spectra and samples sugars composition, where three distinct groups were formed: glycoproteins, on the positive side of CV1; glucuronoxylans, on the negative side; and, between these two groups, but still on the negative side of CV1, xylans and xyloglucans. Fig. 6(b) shows the CCA loadings of the sugars composition data matrix. CV1 is related negatively with Xyl and positively with all other sugars. Comparing Fig. 6(a) and (b), it can be seen that the Xyl of glucuronoxylans and the Ara of glycoproteins are the responsible for the distinction of the FTIR spectra of these cell-wall polymers. Fig. 6(c) shows the CCA loadings of the FTIR spectra data matrix. It can be seen that the wavenumbers characteristic for the distinction of Xyl are in accordance with the results previously obtained with the data set 2. In this data set, only CV1 was interpretable due to the high correlation between the two domains (0.93); on the other hand, CV2 had a very weak correlation (0.40) and, therefore, was not analysed.

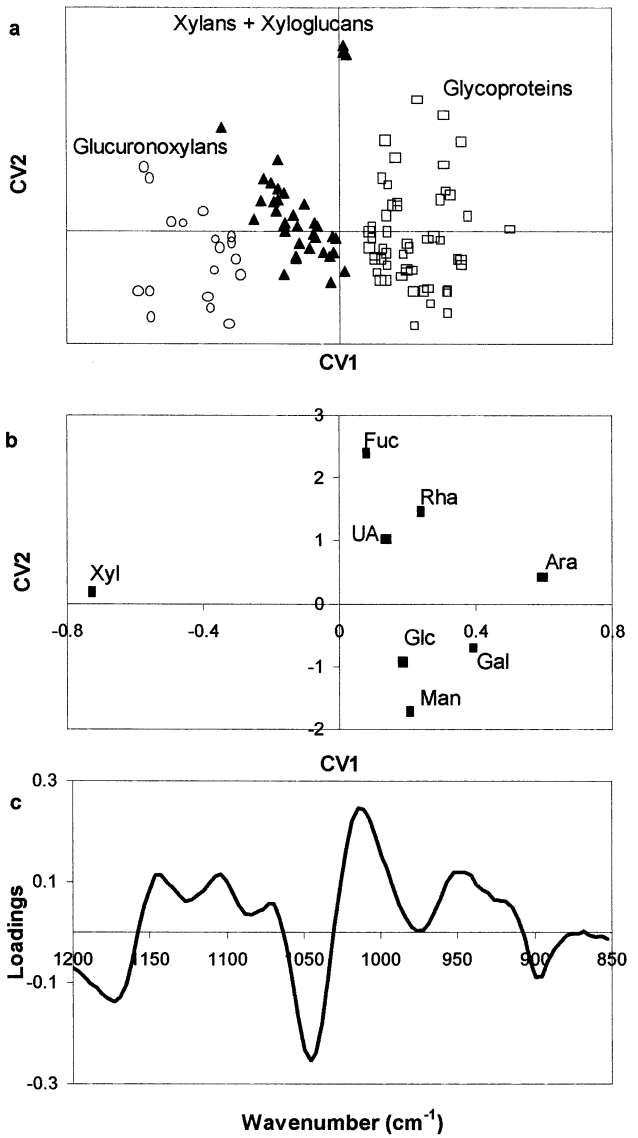

Fig. 6. CCA of data set 3: (a) scores of the spectral data matrix; (b) loadings of the sugars composition data matrix; and (c) loadings of the spectral data matrix.

Calibration model for determination of Xyl.—In order to propose a calibration model and identify the most important wavenumbers for the evaluation of Xyl residues in hemicellulosic samples, a PLS1 was built for data set 3. Four factors, estimated by internal cross-validation (leave-one-out procedure), were required to obtain a predictive ability. Fig. 7(a) shows the B coefficients vector plot with which it is possible to characterise the most important wavenumbers for prediction of Xyl. Positive bands, at 1173, 1041, 972 and 900 cm^{-1}, are related to samples with high Xyl content; the band at 1014 cm^{-1} is negatively correlated to the Xyl content. This plot confirms the results obtained with CCA (Fig. 6(c)). The regression curve obtained (Fig. 7(b)) had a coefficient of determination (R^2) of 0.966 and a root mean square error of prediction of 10.7%; the 95% confidence limits are plotted for each determination. These results show that, although some dispersion is observed in some spectra, FTIR spectroscopy can provide a quick evaluation of the relative content of Xyl in olive hemicellulosic samples.

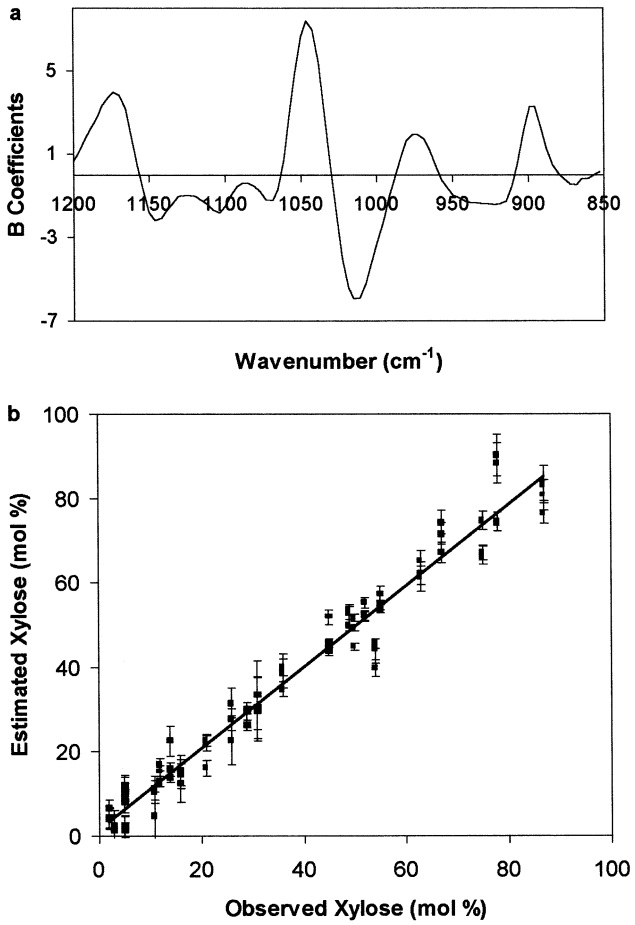

Fig. 7. Calibration model for the determination of xylose-PLS1 with 4 PCs. (a) B coefficients plot; and (b) calibration curve.

Acknowledgements

The authors acknowledge the support of the Program of Cooperation of the Portuguese French Embassy and JNICT, the Program FAIR CT97-3053, the Research Unit 62/94, and the University of Aveiro. They are also grateful to Fernando Nunes and Rita Silva for the FTIR analysis and to Professor Armando Duarte for FTIR apparatus facilities.

References

[1] M.C. McCann, M. Hammouri, R. Wilson, P. Belton, K. Roberts, *Plant Physiol.*, 100 (1992) 1940–1947.

[2] C. Boeriu, T. Stolle-Smits, C. van Dijk, *Pol. J. Food Nutr. Sci*, 7/48 (1998) 257S–266S.

[3] E.K. Kemsley, P.S. Belton, M.C. McCann, S. Ttofis, R.H. Wilson, I. Delgadillo, *Food Control*, 5 (1994) 241–243.

[4] P.S. Belton, E.K. Kemsley, M.C. McCann, S. Ttofis, R.H. Wilson, I. Delgadillo, *Food Chem.*, 54 (1995) 437–441.

[5] M.C. McCann, N.C. Carpita, W-D. Reiter, L. Chen, K. Roberts, H. Hofte, M. Fagard, C. Jeffries, N.J. Stacey, R.H. Wilson, Abstracts and Programme of the 8th International Cell Wall Meeting, Norwich, 1998, 3.01.

[6] M.A. Coimbra, A. Barros, M. Barros, D.N. Rutledge, I. Delgadillo, *Carbohydr. Polym.*, 37 (1998) 241–248.

[7] R.R. Selvendran, M.A. O'Neill, in D. Glick (Ed.), *Methods of Biochemical Analysis*, Vol. 32, Wiley, New York, 1985, pp. 25–153.

[8] M.A. Coimbra, I. Delgadillo, K.W. Waldron, R.R. Selvendran, in H.F. Linskens, J.F. Jackson (Eds.), *Modern Methods of Plant Analysis*, Vol. 17, Springer-Verlag, Berlin, 1996, pp. 19–44.

[9] N. Blumenkrantz, G. Asboe-Hansen, *Anal. Biochem.*, 54 (1973) 484–489.

[10] T.M.C.C. Filizetti-Cozzi, N.C. Carpita, *Anal. Biochem.*, 197 (1991) 157–162.

[11] B. Quemener, M. Lahaye, J.-F. Thibault, *Carbohydr. Polym.*, 20 (1993) 87–94.

[12] M.E. Quigley, H.N. Englyst, *Analyst*, 119 (1994) 1511–1518.

[13] M.A.C. Leitão, M.L. Alarcão Silva, M.I.N. Januário, H.N. Azinheira, *Carbohydr. Polym.*, 26 (1995) 165–169.

[14] S.C. Fry, *The Growing Plant Cell Wall: Chemical and Metabolic Analysis*, Longman, Harlow, UK, 1988.

[15] M.A. Coimbra, K.W. Waldron, R.R. Selvendran, *Carbohydr. Res.*, 252 (1994) 245–262.

[16] M.A. Coimbra, K.W. Waldron, I. Delgadillo, R.R. Selvendran, *J. Agric. Food Chem.*, 44 (1996) 2394–2401.

[17] R.J. Redgwell, R.R. Selvendran, *Carbohydr. Res.*, 157 (1986) 183–199.

[18] R.R. Selvendran, J.F. March, S.G. Ring, *Anal. Biochem.*, 96 (1979) 282–292.

[19] A.B. Blakeney, P.J. Harris, R.J. Henry, B.A. Stone, *Carbohydr. Res.*, 113 (1983) 291–299.

[20] P.J. Harris, A.B. Blakeney, R.J. Henry, B.A. Stone, *J. Assoc. Off. Anal. Chem.*, 71 (1988) 272–275.

[21] D.N. Rutledge, P. McIntyre, *Chemom. Intell. Lab. Sys.*, 16 (1992) 95–101.

[22] I.T. Jolliffe, *Principal Component Analysis*, Springer-Verlag, New York, 1986.

[23] W.J. Krzanowski, *Principal Multivariate Analysis: A Users Perspective*, Clarendon Press, Oxford, 1988.

[24] H. Hove, Y-Z. Liang, O.M. Kvalheim, *Chemom. Intell. Lab. Sys.*, 27 (1995) 33–40.

[25] P. Geladi, B.R. Kowalski, *Anal. Chim. Acta*, 185 (1986) 1–17.